TITLE
An Optimization Approach to Inverse Dynamics Provides Insight as to the Function of the Biarticular Muscles During Vertical Jumping

AUTHOR
Cleather, Daniel J.; Goodwin, Jon E.; Bull, Anthony M. J.

JOURNAL
Annals of Biomedical Engineering

DATE DEPOSITED
17 May 2012

An Optimization Approach to Inverse Dynamics Provides Insight as to the Function of the Biarticular Muscles During Vertical Jumping.

Abstract

Traditional inverse dynamics approaches to calculating the inter-segmental moments are limited in their ability to accurately reflect the function of the biarticular muscles. In particular they are based upon the assumption that the net inter-segmental moment is zero and that total joint moments are independent of muscular activity. Traditional approaches to calculating muscular forces from the inter-segmental moments are based upon a consideration of joint moments which do not encapsulate the potential moment asymmetry between segments. In addition, traditional approaches may artificially constrain the activity of the biarticular muscles. In this study, an optimization approach to the simultaneous inverse determination of inter-segmental moments and muscle forces (the 1 step method) based upon a consideration of segmental rotations was employed to study vertical jumping and contrasted with the more traditional 2 step approach of determining inter-segmental moments from an inverse dynamics analysis then muscle forces using optimization techniques. The 1 step method resulted in significantly greater activation of both the monoarticular and biarticular musculature which was then translated into significantly greater joint contact forces, muscle powers and inter-segmental moments. The results of this study suggest that traditional conceptions of inter-segmental moments do not completely encapsulate the function of the biarticular muscles and that joint function can be better understood by recognising the asymmetry in inter-segmental moments.

Keywords: musculoskeletal modelling, muscle force, joint contact force, muscle power, inter-segmental moments

Introduction

A combination of inverse dynamics methodology and static optimization techniques have been widely employed to estimate the muscular forces that produce human movement. This approach can be characterized as a 2 step method. In the first step the human body is modelled as a series of linked rigid segments. Inverse dynamics are used to calculate the inter-segmental moments observed during a given movement by consideration of segmental factors alone. Subsequently, in the second step, the geometry of the musculoskeletal system is added and optimization techniques are employed to estimate the muscular forces produced during the movement, based on a description of the moment arms and lines of actions of the muscles, and the assumption that the muscles are the sole producers of the inter-segmental joint moments. The optimization problem therefore consists of determining the muscular forces that produce the moments that have been previously calculated during the inverse dynamics analysis.

The inverse dynamics method is based upon using the Newton-Euler equations of motion. Given the forces and moments on the most distal end of a linked chain of rigid body segments and an assessment of the 3D kinematics of the most distal segment, the Newton-Euler equations of motion can be applied to the segment to calculate the force and moment at the proximal end of the segment. This then provides the force and moment on the distal end of the adjacent (proximal) segment, and if the 3D kinematics of this segment are known then the force and moment at the proximal end of this segment can be calculated by the same methodology. In this way, the inter-segmental forces and moments can be calculated

iteratively by moving from distal to proximal along a kinetic chain of linked rigid body segments.

A characteristic of the traditional approach to inverse dynamics is a result of the iterative nature of the method. The moment at the proximal joint of a body segment is uniquely determined by the moment at the distal joint, in combination with a consideration of the inter-segmental forces impressed on the segment and its angular motion. This approach is appropriate for the movement of a series of linked body segments which are actuated by monoarticular muscle function however, a sequential approach to calculating the inter-segmental moments does not fully reflect the potential role of the biarticular muscles. In particular, the iterative approach assumes that the moment expressed at the proximal end of a segment is opposed by an equal moment at the distal end of the adjacent segment by muscular activity. Clearly, the existence of the biarticular muscles permits only a proportion of the moment at the proximal end of a segment to be opposed by muscle activity at the adjacent segment, whereas the moment created by the biarticular muscles will be opposed at non-adjacent segments. This means that the inter-segmental moment can be asymmetric, that is different moments can act at the two ends of adjacent segments creating a net inter-segmental moment that is non-zero. In order to better understand the nature of joint moments it is helpful to define a number of different inter-segmental or joint moments. Four different moments could be considered to act at a joint. Firstly, the notional joint moment ($\hat{M}_J$) which is defined to be rotation moment impressed by all structures that cross the joint. Secondly, the proximal ($\hat{M}_P$) and distal ($\hat{M}_D$) joint moments which represent the rotations created by all structures that cross the joint and insert onto the proximal or distal segment respectively. Finally, the inter-segmental moment ($\hat{M}_S$) can be defined to be the moment created by only

the structures that cross the joint and insert upon both the proximal and distal segment of the joint (that is the monoarticular muscles).

Figure 1 illustrates a joint that is spanned by both monoarticular and biarticular muscles. $\hat{F}^m$ and $\hat{r}^m$ represent the force and moment arms of the monoarticular muscles, $\hat{F}_1^b$ and $\hat{r}_1^b$ the force and moment arms of the biarticular muscles that insert onto the distal segment and $\hat{F}_2^b$ and $\hat{r}_2^b$ the force and moment arms of the biarticular muscles that insert onto the proximal segment. It is readily apparent that:

$$\hat{M}_J = \hat{r}^m \times \hat{F}^m + \hat{r}_1^b \times \hat{F}_1^b + \hat{r}_2^b \times \hat{F}_2^b \quad (1)$$

$$\hat{M}_D = \hat{r}^m \times \hat{F}^m + \hat{r}_1^b \times \hat{F}_1^b \quad (2)$$

$$\hat{M}_P = \hat{r}^m \times \hat{F}^m + \hat{r}_2^b \times \hat{F}_2^b \quad (3)$$

$$\hat{M}_S = \hat{r}^m \times \hat{F}^m \quad (4)$$

Combining Equations 1 to 4 gives:

$$\hat{M}_J = \hat{M}_P + \hat{M}_D - \hat{M}_S \quad (5)$$

As the traditional iterative approach to the inverse dynamics problem of calculating joint moments precludes biarticular muscle function, Equations 1 and 4 are equivalent for the traditional approach. This also leads to the conception that joint moments are independent of muscle forces. However, as can be seen from Figure 1, the inclusion of biarticular muscle function allows non-adjacent segments to be involved in the maintenance of moment equilibrium at a joint. Thus, a more detailed free body diagram implies that joint moments are dependent on muscular activity and that the inclusion of biarticular muscles results in an indeterminate problem, as the muscular activity of mono and biarticular muscles will determine the proportion of the moment that is opposed by adjacent and non-adjacent segments. To accommodate the function of the biarticular muscles it is therefore necessary to solve the equations of motion of a given linked chain of rigid body segments simultaneously. However, formulating an inverse dynamics problem that includes biarticular muscle function in this way significantly increases the complexity of the problem, mainly due to the introduction of this additional indeterminacy. These complexities have led the vast majority of researchers to employ the sequential inverse dynamics method in order to calculate inter-segmental joint moments.

Generally during the inverse dynamics process, the inter-segmental moments are calculated in the body fixed local coordinate system of the segment[9,33,37]. The inverse dynamics process therefore entails a series of coordinate transformations between the global coordinate system (GCS) and the local coordinate system (LCS) of each segment. Alternatively, Dumas and colleagues[8] have presented an inverse dynamics method based on the use of unit quaternions and wrench notation that allows all the calculations to be performed in the GCS. This approach is clearly advantageous in reducing the computational complexity of the process.

Both approaches to the inverse dynamics problem are rooted in classical mechanics and therefore theoretically equivalent and they can thus be used interchangeably[4].

The reduced complexity of the inverse dynamics solution of Dumas and colleagues[8] presents new opportunities for the analysis of human movement. In particular, it is possible to write equations of motion in the GCS that comprise a description of both the segmental motion and the musculoskeletal geometry. Although this system of equations will be indeterminate due to both the large number of force actuators and the presence of biarticular muscles (as seen before), the simultaneous solution of these equations by optimization techniques would permit an inverse dynamics solution that more fairly represents the role of the biarticular muscles. Additionally, the solution of the equations of motion allows the muscular forces to be found independently of the joint moments, and the precise involvement of the biarticular muscles in redistributing joint moments to be determined by the same optimization cost function used to determine the muscle forces producing the observed moments.

Traditional optimization solutions rely upon a consideration of the action of muscles on joints and the assumption that muscular joint moments create the calculated inter-segmental moments. These inter-segmental moments are then decomposed into individual muscle forces, based upon the muscle elements that cross the joint. This approach does not recognize the fact that the biarticular muscles are not physically connected to all the segments that they cross. Equally, the approach assumes that the net inter-segmental moment is zero, whereas it has already been seen that the presence of the biarticular muscles results in the possibility of the net inter-segmental moment being non-zero. Instead, it may be more

appropriate to formulate the equations of motion utilized in the optimization process in terms of the rotation of segments thereby permitting asymmetry in the inter-segmental moments.

The biarticular muscles have received considerable attention within the biomechanics literature. Despite this their function during movement is not well understood. A number of researchers have sought to understand the function of the biarticular muscles by employing the combination of inverse dynamics and optimization techniques[10,24,32]. The majority of this work is based upon finding the inverse dynamics solution using traditional techniques and then performing sensitivities on the effect of the biarticular muscles on the optimization solution. This approach is limited by the fact that the inverse dynamics method of finding the inter-segmental moments neglects the role of the biarticular muscles as seen earlier. A notable exception to this is the upper extremity model of Raikova[27,26] who formulated an indeterminate description of the upper extremity comprising 10 muscles (including 4 biarticular muscles) in the sagittal plane, and then used the method of Lagrange multipliers to find the optimal solution to the indeterminate problem. Despite the success of Raikova's pioneering work in 2D, later researchers have not employed similar methodologies to concurrently determine inter-segmental moments and muscle forces. The purpose of this study was therefore to use the inverse dynamics solution of Dumas and colleagues[8] to write 3D equations of motion of the lower limb incorporating a description of the musculoskeletal geometry and to explore the use of standard optimization techniques in solving this indeterminate problem. The clinical aim of the study was to use this new technique to explore the postulated role of the biarticular muscles in transferring energy between segments. In particular, a number of groups have reported that the biarticular muscles act to transfer energy between segments during jumping and landing [11,17,25,32], thus vertical jumping was considered to represent an appropriate model to explore biarticular muscle function.

Materials and Methods

This study employed a musculoskeletal model of a right lower limb. The musculoskeletal model is a linked rigid segment model consisting of four segments (foot, calf, thigh and pelvis), articulated by three ball and socket joints at the ankle, knee and hip. A more detailed description of the model has previously been provided[5].

Twelve athletic males (mean age 27.1 ± 4.3 years; mean mass 83.7 ± 9.9 kg) participated in this study. The study was approved by the Institutional Review Board of St Mary's University College. After providing informed consent and performing a standardized warm up, the subjects performed up to 5 maximum vertical jumps. The highest jump was chosen for analysis (mean height 0.38 ± 0.05 m). The data was acquired using standard motion capture (Vicon MX System, Vicon Motion Systems Ltd, Oxford, UK) and force plate techniques (Kistler Type 9286AA, Kistler Instrumente AG, Winterthur, Switzerland) at 200 Hz. The motion capture system established the position of reflective markers placed on key anatomical landmarks[28,29]. A fifth order Woltring filter[34] was used to smooth the raw data and then the position of the markers was transformed into the translations and rotations that represented the position and orientation of each segment of the model using the method of Horn[14]. The methods of Dumas and colleagues[8] were used to calculate the kinematics of each segment based on the anthropometric model of de Leva[7].

The musculoskeletal geometry of the model was based on the cadaveric data of Horsman and colleagues[15]. Subject-specific scaling of the muscle model was performed at the segmental level by comparing the anthropometry of the Horsman data and that of each subject to create

linear scaling factors along each axis of the LCS of each segment. The data of Horsman was also used to determine the location of the patella relative to the femur. The rotation of the patella with respect to the femur was based on the data of Nha and colleagues[19] whereby spline interpolation (using "Numerical Recipes in C++"[23]) was used to calculate the rotation of the patella for any given knee flexion angle. The wrapping of the quadriceps muscle groups around the femoral condyles at deeper knee flexion angles was achieved by the insertion of wrapping points for each quadriceps muscle element. The patella was considered to act as a rigid lever and thus the contact position of the posterior surface of the patella on the femoral condyles was assumed to translate superiorly and inferiorly on the posterior surface of the patella in order for the patella to maintain its force and moment equilibrium. The musculoskeletal model was used to calculate the line of action and moment arm of each muscle element based upon the instantaneous body posture for use in the optimization.

Five distinct solutions of each data set were sought. The first two entailed using the traditional sequential 2 step approach (TRAD) of performing an inverse dynamics analysis to find joint moments then performing an optimization to calculate muscle forces. In the first of these, a solution was sought based on a modified version of the Horsman et al.[15] muscle set consisting of solely monoarticular muscles (TRADM) whereas the second was based upon the complete Horsman data set incorporating biarticular muscles (TRADB). The modified Horsman muscle set was created by dividing each biarticular muscle into two independent monoarticular muscles[10], thus the optimization produced two different force values for each biarticular muscle (the larger value is presented in the results section). The remaining three permutations consisted of different implementations of a new 1 step approach, whereby the inverse dynamics solution was found simultaneously with the determination of muscle forces. In the first of these, a solution was sought based on the monoarticular muscle set (MONO).

In the remaining two approaches, the new method was implemented incorporating the complete musculoskeletal geometry of Horsman. In the first of these solutions the maximum possible muscle force was according to Horsman (BI), whereas in the second solution the maximum possible muscle force was doubled for selected biarticular muscles (gastrocnemius, biarticular hamstrings and rectus femoris) in order to assess the sensitivity of the model to changes in the function of the biarticular muscles (BIH).

Traditional Approach (2 Step)

For the TRAD approach, the method of Dumas and colleagues[8] was used to find the inverse dynamics solution. According to the method, the equations of motion can be written as:

$$\begin{bmatrix} \hat{S}_i \\ \hat{M}_i \end{bmatrix} = \begin{bmatrix} m_i E_{3\times3} & 0_{3\times3} \\ m_i \tilde{c}_i & I_i \end{bmatrix} \begin{bmatrix} \hat{a}_i - \hat{g} \\ \ddot{\hat{\theta}}_i \end{bmatrix} + \begin{bmatrix} 0_{3\times1} \\ \dot{\hat{\theta}}_i \times I_i \dot{\hat{\theta}}_i \end{bmatrix} + \begin{bmatrix} E_{3\times3} & 0_{3\times3} \\ \tilde{d}_i & E_{3\times3} \end{bmatrix} \begin{bmatrix} \hat{S}_{i-1} \\ \hat{M}_{i-1} \end{bmatrix} \qquad (6)$$

where:

i - segment number or joint number (numbering from distal to proximal)

$\hat{S}_i$ - proximal inter-segmental forces

$\hat{S}_{i-1}$ - distal inter-segmental forces

$\hat{M}_i$ - proximal inter-segmental moments (notional joint moments)

$\hat{M}_{i-1}$ - distal inter-segmental moments (notional joint moments)

I_i - inertia tensor

$\dot{\hat{\theta}}_i$ - angular velocity about COM

$\ddot{\hat{\theta}}_i$ - angular acceleration about COM

$\hat{a}_i$ - linear acceleration of COM

m_i - segment mass

E_{3x3} - identity matrix

$\hat{c}$ - vector from the proximal joint to the segment COM

$\hat{d}$ - vector from the proximal to the distal joint

and $\tilde{c}$ represents the skew symmetric matrix of a 3D vector:

$$\tilde{c} = \begin{pmatrix} 0 & -c_3 & c_2 \\ c_3 & 0 & -c_1 \\ -c_2 & c_1 & 0 \end{pmatrix} \quad (7)$$

The indeterminate problem of resolving notional joint moments into individual muscle forces at each joint can be expressed by Equation 8.

$$\sum_{j=1}^{N} F_j \cdot \hat{n}_{ji} \times \hat{r}_{ji} = \hat{M}_i \quad (8)$$

This was solved by optimizing the objective function of Crowninshield and Brand[6] which is thought to maximise muscular endurance by minimizing muscle stress. The work of Crowninshield and Brand suggests that by raising muscle stress to increasingly higher powers an optimal solution path can be defined which converges on the solution which minimizes muscle stress. Although Crowninshield and Brand suggest that an exponent between 2 and 4 may be appropriate, we have found that optimal force-sharing in our model is found by raising muscle stress to a higher power than is typical within the literature[5].

$$\min_{F_j} f = \sum_{j=1}^{K} \left(\frac{F_j}{F_{\max_j}} \right)^{30} \tag{9}$$

Subject to the constraints that:

$$0 \le F_j \le F_{\max_j} \tag{10}$$

N - number of muscles spanning the joint

F_j - individual muscle force

$F_{\max_j}$ - maximum possible muscle force

$\hat{n}_{ji}$ - line of action of muscle j about joint i

$\hat{r}_{ji}$ - moment arm of muscle j about joint i

K - total number of muscles

New Approach (1 Step)

In the 1 step approach, the inter-segmental forces were first determined in the GCS using the standard approach. The moment part of the wrench equations of Dumas et al.[8] was then used to formulate an alternative indeterminate problem, that did not explicitly include the inter-segmental joint moments (Equation 11). The key kinematic and kinetic variables used in Equation 11 are depicted in Figure 2.

$$\begin{bmatrix} \hat{S}_i \\ \sum_{j=1}^{K} F_j \cdot \hat{n}_{ji} \times \hat{r}_{ji} - \sum_{j=1}^{K} F_j \cdot \hat{n}_{j(i-1)} \times \hat{r}_{j(i-1)} \end{bmatrix} = \begin{bmatrix} m_i E_{3\times3} & 0_{3\times3} \\ m_i \tilde{c}_i & I_i \end{bmatrix} \begin{bmatrix} \hat{a}_i - \hat{g} \\ \ddot{\hat{\theta}}_i \end{bmatrix} + \begin{bmatrix} 0_{3\times1} \\ \dot{\hat{\theta}}_i \times I_i \dot{\hat{\theta}}_i \end{bmatrix} + \begin{bmatrix} E_{3\times3} & 0_{3\times3} \\ \tilde{d}_i & E_{3\times3} \end{bmatrix} \begin{bmatrix} \hat{S}_{i-1} \\ \hat{M}_{i-1} \end{bmatrix} \quad (11)$$

Where $\hat{M}_{i-1}$ was set to zero for i>1. This optimization problem was then solved using the same cost function as for the TRAD method.

It is apparent that the two methodologies are significantly different with regards to the optimization approach. Most notably, the 2 step method is based upon finding the muscle forces that produce the observed joint moments in contrast to the 1 step method which calculates the muscles forces that produce the observed segmental rotations. In order to better contrast the two methods, the notional joint moment was calculated for the 1 step

method by considering the moment produced by each muscle element (mono or biarticular) that crossed a given joint based upon the definition given in the introduction.

In the first instance, the upper bound of each muscle was based upon the physiological cross sectional area provided by the Horsman et al.[15] data set (which was doubled to represent the fact that the subjects were from an athletic population as was proposed by Yamaguchi[35]) then multipled by a maximum muscle stress of 3.139×10^5 N/m^2 [35]. This approach resulted in a viable solution for the vast majority of the frames for 6 of the 12 subjects. A limited number of frames either immediately before take-off or after landing were not able to produce a solution based upon this upper bound, in which case the upper bound was increased in order to permit a solution. For the remaining subjects, the upper bound was increased until a viable solution for the majority of the frames could be found. The highest upper bound used in this study equates to a maximum physiological cross-sectional area 4.5 times greater than the figure provided by Horsman. The same upper bound was used across all cases for each subject. Post optimization analysis of the muscle forces calculated revealed that the increased upper bound was only utilized by a limited number of the smaller muscles and therefore did not markedly increase the overall activation produced by the model. This problem was therefore considered to be a result of the difficulty in creating a subject-specific geometry, and the magnitude of the produced muscle and joint forces assumed to be both valid and comparable.

The muscle forces calculated were in turn employed to calculate internal joint forces. These included the calculation of ankle joint contact force, patellofemoral joint contact force (PFJ),

tibiofemoral joint contact force (TFJ), anterior and posterior shear (AS and PS) and hip joint contact force. The internal knee forces calculated are depicted in Figure 3.

Finally, the muscle power of the biarticular muscles was calculated using the method of Zajac and colleagues[36]:

$$\hat{p}_{ji} = \hat{J}_{ji} \cdot \hat{\omega}_i \qquad (12)$$

$\hat{p}_{ji}$ - muscle power of muscle j at joint i

$\hat{J}_{ji}$ - moment of muscle j at joint i

$\hat{\omega}_i$ - angular velocity of joint i

The net joint power of a biarticular muscle was considered to be the sum of the muscle powers developed by the muscle at each joint.

Paired t-tests were used to test the hypothesis that there are differences between the muscle forces, joint contact forces, muscle powers and joint moments calculated using the different techniques by comparing each biarticular condition to its monoarticular analogue. Additionally, the BI and BIH methods were compared to TRADB to ascertain the difference between the representation of the biarticular muscles in the 1 and 2 step approaches. Statistical significance was set at alpha = 0.05.

Results

A successful solution of the optimization problem was found for over 99% of the analyzed frames, and all methods were able to produce a solution. Tables 1 and 2 present the peak muscle forces calculated based upon the five methods. Muscle forces were markedly similar between the two monoarticular cases (TRADM and MONO). All three biarticular methods predicted a reduction in gastrocnemius force for jumping and an increase in hamstrings force for both jumping and landing, although notably the BI and BIH methods always predicted higher activations than the TRAD method. The TRADB method suggested a decreased activation of rectus femoris in both jumping and landing and gastrocnemius during landing, whereas the BI and BIH methods indicated increased rectus femoris and gastrocnemius loading in these cases. All biarticular cases predicted higher total activation of the hip and knee extensors and higher activation of the monoarticular musculature at all three joints. At a subject level, there were often large differences between the activation patterns predicted across the different cases (Figure 4).

The differences in the mean peak joint forces (see Tables 3 and 4) were consistent with the differences in muscular activation. Specifically there were few differences between the monoarticular cases whereas the biarticular cases had mainly greater joint contact forces when compared to their monoarticular analogues. The BI and BIH methods generally resulted in significantly greater shear forces at the knee, whereas the TRADB method did not differ markedly from its monoarticular analogue.

The calculation of muscle power demonstrated that the gastrocnemius, rectus femoris and biarticular hamstrings consistently functioned to produce positive power at one joint while simultaneously producing negative power at the other (Figure 5). The net power of these muscles was positive during jumping and negative during landing. The peak positive muscle power during jumping, and peak negative muscle power during landing was greater in the BI and BIH methods than the TRADB method (Tables 5 and 6).

The joint moments calculated based upon the TRAD and MONO methods were virtually identical (Table 7). In addition, the moments calculated at the ankle were in agreement across all methods. The notional sagittal plane moments for the knee and hip calculated for the BI and BIH methods were generally in close agreement however, they tended to diverge towards the peak values (Figure 6). The degree of divergence was often greater at the hip than at the knee.

Discussion

In this study a new approach to calculating joint moments and muscle forces using optimization techniques was described. The methodology was based on using the quaternion and wrench notation implementation of the inverse dynamics method, described by Dumas and colleagues[8], to formulate an indeterminate problem relating the muscle forces to the observed kinetic and kinematic variables describing the movement of the body segments. Optimization techniques were used to estimate muscle forces, and then the moments were calculated as the resultant of the muscle forces given the known musculoskeletal geometry.

As the foot segment represents the terminal link of the kinetic chain, the ankle moment is uniquely determined by the kinematics of the foot and the ground reaction force. This was supported in the results of this study, as all methods yielded the same ankle moments. More significantly, in a rigid linked chain actuated entirely by monoarticular muscles, the inverse dynamics solution at all joints is uniquely determined by the segment kinematics and the ground reaction force. To this end, the moments calculated by the TRADM and MONO methods should theoretically be the same, as was the case in this study. Equally, the similarity between the optimization problems posed in the TRADM and MONO approaches suggests a similarity in the predicted muscle forces, a prediction which was also supported in the current study. These findings support the validity of the approach and provide some verification as to the veracity of the implementation.

The introduction to this article suggested that the traditional approach to the calculation of muscle forces by optimization techniques does not fully reflect the role of the biarticular muscles. In this study it was found that the 1 step approach yielded different joint moments. This is due to the fact that in the more explicit free body diagram used in the 1 step approach, the notional joint moments are dependent on the calculated muscle forces and that the biarticular muscles may have differing moment arms at the two joints that they cross. Figure 7 presents a comparison of the 1 and 2 step approaches to calculating joint moments. It is worth noting that although the 2 step approach is not dependent upon muscle forces, it can be represented as the action of a system of monoarticular muscles. This convention is chosen to allow comparison between the two approaches. The nomenclature employed in Figure 7 is as follows:

$\hat{S}_i$ - inter-segmental forces

$\hat{M}_0$ - distal external moment

$\hat{F}_i^m$ - total force due to monoarticular muscles at joint i

$\hat{r}_i^m$ - moment arm of monoarticular muscles at joint i

$\hat{F}^b$ - force due to biarticular muscle action

$\hat{r}_i^b$ - moment arm of biarticular muscle at joint i

For the 1 and 2 step approaches, considering segment 1 and using the moment part of Equation 11 it can be seen that:

$$\hat{r}_1^m \times \hat{F}_1^m + \hat{r}_1^b \times \hat{F}^b = \begin{bmatrix} m_1\tilde{c}_1 & I_1 \end{bmatrix} \begin{bmatrix} \hat{a}_1 - \hat{g} \\ \ddot{\hat{\theta}}_1 \end{bmatrix} + \dot{\hat{\theta}}_1 \times I_1 \dot{\hat{\theta}}_1 + \begin{bmatrix} \tilde{d}_1 & E_{3\times 3} \end{bmatrix} \begin{bmatrix} \hat{S}_0 \\ \hat{M}_0 \end{bmatrix} \quad (13)$$

$$\hat{r}_1^{m\prime} \times \hat{F}_1^{m\prime} = \begin{bmatrix} m_1\tilde{c}_1 & I_1 \end{bmatrix} \begin{bmatrix} \hat{a}_1 - \hat{g} \\ \ddot{\hat{\theta}}_1 \end{bmatrix} + \dot{\hat{\theta}}_1 \times I_1 \dot{\hat{\theta}}_1 + \begin{bmatrix} \tilde{d}_1 & E_{3\times 3} \end{bmatrix} \begin{bmatrix} \hat{S}_0 \\ \hat{M}_0 \end{bmatrix} \quad (14)$$

Hence:

$$\hat{r}_1^m \times \hat{F}_1^m + \hat{r}_1^b \times \hat{F}^b = \hat{r}_1^{m\prime} \times \hat{F}_1^{m\prime} \quad (15)$$

Similarly, by considering segment 2:

$$\hat{r}_2^m \times \hat{F}_2^m - \hat{r}_1^m \times \hat{F}_1^m = \begin{bmatrix} m_2\tilde{c}_2 & I_2 \end{bmatrix} \begin{bmatrix} \hat{a}_2 - \hat{g} \\ \ddot{\hat{\theta}}_2 \end{bmatrix} + \dot{\hat{\theta}}_2 \times I_2 \dot{\hat{\theta}}_2 + \hat{d}_2 \times \hat{S}_1 \quad (16)$$

$$\hat{r}_2^{m\prime} \times \hat{F}_2^{m\prime} - \hat{r}_1^{m\prime} \times \hat{F}_1^{m\prime} = \begin{bmatrix} m_2\tilde{c}_2 & I_2 \end{bmatrix} \begin{bmatrix} \hat{a}_2 - \hat{g} \\ \ddot{\hat{\theta}}_2 \end{bmatrix} + \dot{\hat{\theta}}_2 \times I_2 \dot{\hat{\theta}}_2 + \hat{d}_2 \times \hat{S}_1 \quad (17)$$

And:

$$\hat{r}_2^{m\prime} \times \hat{F}_2^{m\prime} = \hat{r}_1^{m\prime} \times \hat{F}_1^{m\prime} + \hat{r}_2^m \times \hat{F}_2^m - \hat{r}_1^m \times \hat{F}_1^m \quad (18)$$

Now using Equations 1, 15 and 18:

$$\hat{M}_{J_2}{}' = \hat{r}_2^m \times \hat{F}_2^m + \hat{r}_1^b \times \hat{F}^b \quad (19)$$

Now by definition:

$$\hat{M}_{J_2} = \hat{r}_2^m \times \hat{F}_2^m + \hat{r}_2^b \times \hat{F}^b \quad (20)$$

Thus it is apparent that $\hat{M}_{J_2}$ is not equal to $\hat{M}_{J_2}{}'$ when the moment arms of the biarticular muscles at each end of the segment are different. This result explains the findings of this study that the notional joint moments are different.

A major consequence of the traditional approach is therefore that during the optimization process, the activation of the biarticular muscles is artificially constrained, as the sum of the monoarticular and biarticular muscle moments must be equal to the calculated inter-segmental moment. In contrast, the new approach is not constrained by an assumption as to the joint moment, and thus differing activations of the biarticular muscles contribute to alter the notional joint moment in comparison to the traditional approach. In this study, the practical consequence of this was that the biarticular muscles were permitted to have a significantly higher activation than in the TRADB method. Due to the formulation of the indeterminate problem in the 1 step method the activation of the biarticular muscles is governed by the cost function chosen in the optimization. That is, the optimal solution of the indeterminate problem is the one which minimizes muscle stress. Of course, the total level of muscle stress found in the BI and BIH methods may still be higher than that found in the TRADB approach due to the difference in the optimization problem. The assumption that the coordination of biarticular muscle function is due to an imperative to minimize muscle stress is supported by the work of Prilutsky and colleagues[24] who found that the recruitment of the biarticular muscles of the lower limb during a back lift task was consistent with a strategy to minimize muscle force, stress and fatigue in a 2D model and also with work demonstrating improved running economy associated with increased biarticular co-activation[12,13].

The magnitude of the joint moments predicted by the TRAD method and the temporal pattern of the joint moments predicted by all methods were in agreement with those found in previous work[2,18,31]. The temporal pattern of muscular activation found in this study exhibited some variation between subjects and cases, but the general trends were also in agreement with previous research employing both experimental and in silico methods[1,2,3,20,21]. In particular, the attainment of peak activation in the monoarticular joint extensors followed a

broadly proximal to distal trend[20,21] with the biggest variation found in relative timings of the knee and hip musculature – a variation which is found within the literature[2,3]. The principle difference in the timing of muscular activity between the 1 and 2 step methods is that the 1 step method tended to suppress the activity of rectus femoris during propulsion with the exception of an impulsive peak immediately prior to takeoff. The muscular forces predicted in this study during landing are in agreement with the work of Pflum and colleagues[22], although the activation of vastus is lower in this work.

In this study, the biarticular cases generally resulted in a greater activation of both the biarticular and monoarticular musculature. Fraysse and colleagues[10] have recently published work analyzing the effect of the biarticular muscles on the calculation of muscular forces during gait using the traditional 2 step approach of inverse dynamics and optimization. Their study is analogous to a comparison of the TRADM and TRADB approaches used in this study. Similar to this study, Fraysse et al. found that when the biarticular function of the muscles was modelled this produced higher activation of the biarticular musculature, however in contrast to the findings of this study this was largely balanced by a commensurate decrease in monoarticular muscle activation. The reason for this difference is probably inherent in the differences between the musculoskeletal models employed. The model of Fraysse and colleagues was constrained to 2 DOF at both the knee and hip, whereas the model employed in this study had 3 DOF at all joints. As a consequence, the model used in this study is more sensitive to the non-sagittal plane moments that the biarticular muscles express across two joints and must therefore be equilibrated by higher monoarticular muscle activation.

The differences between the internal joint contact forces in the biarticular cases when compared to their monoarticular analogues were a consequence of the greater level of muscular activation necessary due to the action of the biarticular muscles. The contact forces were higher in the BI and BIH methods as the activation of the biarticular muscles was not constrained by a calculated joint moment. The difference in contact forces found in this study differ from those suggested by Fraysse and colleagues[10] but this is again a function of the differences in the calculated forces. The results of this study therefore clearly demonstrate the importance of recognizing the function of the biarticular muscles when calculating internal joint forces, and in contrast to the work of Fraysse et al., suggest that the difference in contact forces may be much greater, as the action of the biarticular muscles may be to increase the joint moment, which in turn permits a greater overall level of activation of both biarticular and monoarticular musculature.

It has been suggested that a key function of the biarticular muscles is to transfer energy between the joints[11,16,17,25,30]. In particular, the biarticular muscles are thought to transfer energy from the proximal to distal joints during jumping and from distal to proximal during landing[11,17,25,32]. The pattern of muscle power production observed in this study tends to support this assertion as the biarticular muscles studied tended to produce positive and negative power simultaneously at their respective joints (Figure 5). The results of this study also suggested that the BI and BIH approaches resulted in the biarticular muscles expressing higher net muscle power than in the TRADB case, which may reflect higher energy transfer.

It is interesting to note the temporal pattern in the differences between the TRADB and the BI and BIH methods. In general, there was a closer agreement between the methods when the

magnitude of the joint moments was smaller. At higher joint moments there was a greater tendency for there to be a divergence between the methods which represents a difference in the recruitment of the biarticular musculature. Where the BI or BIH method results in a greater joint moment than the TRADB method this therefore indicates greater activation of the biarticular musculature, which will increase the transfer of energy between joints as the kinematics remain unchanged.

In this study the BIH sensitivity was performed in order to better elucidate the function of the biarticular muscles. Increasing the upper bound of the biarticular muscles increases the likelihood that the force impressed by the biarticular muscles will be increased. This can be characterized as the greater force capability likely to be available to the biarticular muscles should they be functioning eccentrically, isometrically or at lower shortening velocities. However, only small differences were observed between the BI and BIH cases, and these differences were predominantly caused by a small number of subjects. This seems to suggest that for most subjects the size of the selected biarticular muscles relative to the remainder of the musculature of the lower limb was optimized to minimize muscle stress.

A limitation of this study is inherent in the fixed upper bounds employed. When considering the biarticular muscles, which it is argued can function isometrically in transferring energy between segments an assessment of the contractile function of the biarticular muscles is important due to the profound effect of the regime of muscular work (concentric, eccentric or isometric) on the force capabilities of muscle. Future research should further elucidate the function of the biarticular muscles by employing Hill type muscle models to establish the

force upper bounds of the muscles based on changes in length in the muscle-tendon unit. The inclusion of this type of assumption will lead to a more robust assessment of muscular forces.

As noted earlier, the greatest differences between the TRAD and the BI and BIH methods were generally associated with the regions of peak joint moment production. It is worth noting that there is an individual variation in the ease with which the optimization arrives at a viable solution which will in part be influenced by the degree to which the musculoskeletal geometry of the model approximates the actual geometry of the subject. Where a viable solution is harder to find, there is an increased likelihood that the optimal solution will require increased activation[5] and that the optimal solution will therefore require increased activity of the biarticular muscles. It is also worth noting that the optimization problem posed in the 1 step method is of greater complexity than that used in the traditional approach. Although this complexity did not markedly increase the computational time, it did predicate the use of a slightly higher upper bound for 4 of the 12 subjects.

In conclusion, this study presented an optimization based approach to the calculation of muscle forces that better reflects the biarticular function of the muscles of the lower limb. The results of this study demonstrate the key importance of a fair representation of biarticular muscle function. Traditional inverse dynamics approaches are based upon a consideration of joint moments and the assumption that the net inter-segmental moment is zero. Equally, decomposition of the inter-segmental moment into muscle forces is performed without reference to the particular segments to which muscles insert. This study demonstrated that these assumptions may limit the activation of the biarticular muscles. This in turn may understate the magnitude of the joint contact forces and inter-segmental moments during

movement. Future research should therefore employ optimization approaches derived from the equations of motion of the segments. The comparison of the 1 and 2 step approaches also has relevance for clinical practitioners, as it suggests that the popular conception of a joint moment is limited, as it does not represent the moment asymmetry present at joints spanned by biarticular muscles. This asymmetry may be particularly important in the context of injury mechanics.

Acknowledgements

The authors would like to thank the anonymous reviewers for the clarity of their thoughts which greatly increased the transparency of this article.

References

1. Anderson, F. C. and M. G. Pandy. A dynamic optimization solution for vertical jumping in three dimensions. Computer Methods in Biomechanics and Biomechanical Engineering, 2, 201-231, 1999.

2. Bobbert, M. F., K. G. M. Gerritsen, M. C. A. Litjens, and A. J. VanSoest. Why is countermovement jump height greater than squat jump height? Medicine and science in sports and exercise, 28, 1402-1412, 1996.

3. Bobbert, M. F. and J. P. van Zandwijk. Dynamics of force and muscle stimulation in human vertical jumping. Medicine and science in sports and exercise, 31, 303-310, 1999.

4. Cleather, D. J. Forces in the knee during vertical jumping and weightlifting. PhD Thesis, Imperial College London, 2010.

5. Cleather, D. J. and A. M. J. Bull. Lower extremity musculoskeletal geometry effects the calculation of patellofemoral forces in vertical jumping and weightlifting. Proceedings of the Institution of Mechanical Engineers Part H - Journal of Engineering in Medicine, in press, 2010.

6. Crowninshield, R. D. and R. A. Brand. A physiologically based criterion of muscle force prediction in locomotion. Journal of Biomechanics, 14, 793-801, 1981.

7. de Leva, P. Adjustments to Zatsiorsky-Seluyanov's segment inertia parameters. Journal of Biomechanics, 29, 1223-1230, 1996.

8. Dumas, R., R. Aissaoui, and J. A. de Guise. A 3D generic inverse dynamic method using wrench notation and quaternion algebra. Computer methods in biomechanics and biomedical engineering, 7, 159-166, 2004.

9. Dumas, R., E. Nicol, and L. Cheze. Influence of the 3D inverse dynamic method on the joint forces and moments during gait. Journal of Biomechanical Engineering, 129, 786-790, 2007.

10. Fraysse, F., R. Dumas, L. Cheze, and X. Wang. Comparison of global and joint-to-joint methods for estimating the hip joint load and the muscle forces during walking. Journal of Biomechanics, 42, 2357-2362, 2009.

11. Gregoire, L., H. E. Veeger, P. A. Huijing, and G. J. van Ingen Schenau. Role of mono- and bi-articular muscles in explosive movements. International Journal of Sports Medicine, 5, 301-305, 1984.

12. Heise, G. D., D. W. Morgan, H. Hough, and M. Craib. Relationships between running economy and temporal EMG characteristics of bi-articular muscles. International Journal of Sports Medicine, 17, 128-133, 1996.

13. Heise, G. D., M. Shinohara, and L. Binks. Biarticular leg muscles and links to running economy. International Journal of Sports Medicine, 29, 688-691, 2008.

14. Horn, B. K. P. Closed form solution of absolute orientation using unit quaternions. Journal of the Optical Society of America A, 4, 629-642, 1987.

15. Horsman, M. D., H. F. J. M. Koopman, F. C. T. van der Helm, L. Poliacu Prose, and H. E. J. Veeger. Morphological muscle and joint parameters for musculoskeletal modelling of the lower extremity. Clinical Biomechanics, 22, 239-247, 2007.

16. Jacobs, R., M. F. Bobbert, and G. J. V. Schenau. Function of monoarticular and biarticular muscles in running. Medicine and science in sports and exercise, 25, 1163-1173, 1993.

17. Jacobs, R., M. F. Bobbert, and G. J. van Ingen Schenau. Mechanical output from individual muscles during explosive leg extensions: The role of biarticular muscles. Journal of Biomechanics, 29, 513-523, 1996.

18. Lees, A., J. Vanrenterghem, and D. de Clercq. The maximal and submaximal vertical jump: Implications for strength and conditioning. Journal of Strength and Conditioning Research, 18, 787-791, 2004.

19. Nha, K. W., R. Papannagari, T. J. Gill, S. K. Van de Velde, A. A. Freiberg, H. E. Rubash, and G. Li. In vivo patellar tracking: Clinical motions and patellofemoral indices. Journal of Orthopaedic Research, 26, 1067-1074, 2008.

20. Pandy, M. G. and F. E. Zajac. Optimal muscular coordination strategies for jumping. Journal of Biomechanics, 24, 1-10, 1991.

21. Pandy, M. G., F. E. Zajac, E. Sim, and W. S. Levine. An optimal control model for maximum-height human jumping. Journal of Biomechanics, 23, 1185-1198, 1990.

22. Pflum, M. A., K. B. Shelburne, M. R. Torry, M. J. Decker, and M. G. Pandy. Model prediction of anterior cruciate ligament force during drop-landings. Medicine and science in sports and exercise, 36, 1949-1958, 2004.

23. Press, W. H., S. A. Teukolsky, W. T. Vetterling, and B. P. Flannery. Numerical Recipes in C++: The Art of Scientific Computing. Cambridge University Press: Cambridge, NY, 2002, 1002 pp.

24. Prilutsky, B. I., T. Isaka, A. M. Albrecht, and R. J. Gregor. Is coordination of two-joint leg muscles during load lifting consistent with the strategy of minimum fatigue? Journal of Biomechanics, 31, 1025-1034, 1998.

25. Prilutsky, B. I. and V. M. Zatsiorsky. Tendon action of two-joint muscles: Transfer of mechanical energy between joints during jumping, landing, and running. Journal of Biomechanics, 27, 25-34, 1994.

26. Raikova, R. Investigation of the peculiarities of two-joint muscles using a 3 DOF model of the human upper limb in the sagittal plane: An optimization

approach. Computer methods in biomechanics and biomedical engineering, 4, 463-490, 2001.

27. Raikova, R. Prediction of individual muscle forces using Lagrange multipliers method - A model of the upper human limb in the sagittal plane: 1. Theoretical considerations. Computer methods in biomechanics and biomedical engineering, 3, 95-107, 2000.

28. Van Sint Jan, S. Skeletal landmark definitions: Guidelines for accurate and reproducible palpation. University of Brussels, Department of Anatomy (Www.Ulb.Ac.Be/~Anatemb), 2005.

29. Van Sint Jan, S. and U. D. Croce. Identifying the location of human skeletal landmarks: Why standardized definitions are necessary - a proposal. Clinical Biomechanics, 20, 659-660, 2005.

30. van Soest, A. J., A. L. Schwab, M. F. Bobbert, and G. J. van Ingen Schenau. The influence of the biarticularity of the gastrocnemius muscle on vertical jumping achievement. Journal of Biomechanics, 26, 1-8, 1993.

31. Vanezis, A. and A. Lees. A biomechanical analysis of good and poor performers of the vertical jump. Ergonomics, 48, 1594-1603, 2005.

32. Voronov, A. V. The roles of monoarticular and biarticular muscles of the lower limbs in terrestial locomotion. Human Physiology, 30, 476-484, 2004.

33. Winter, D. A. Biomechanics and Motor Control of Human Movement. John Wiley & Sons: Hoboken, NJ, 2005, 344 pp.

34. Woltring, H. J. A Fortran package for generalized, cross-validatory spline smoothing and differentiation. Advances in Engineering Software, 8, 104-113, 1986.

35. Yamaguchi, G. T. Dynamic Modeling of Musculoskeletal Motion: A Vectorized Approach for Biomechanical Analysis in Three Dimensions. Springer: New York, NY, 2001, 257 pp.

36. Zajac, F. E., R. R. Neptune, and S. A. Kautz. Biomechanics and muscle coordination of human walking Part I: Introduction to concepts, power transfer, dynamics and simulations. Gait and Posture, 16, 215-232, 2002.

37. Zatsiorsky, V. M. Kinetics of Human Motion. Human Kinetics: Champaign, IL, 2002, 672 pp.

Table 1. Peak muscle forces (× BW) calculated during vertical jumping for selected muscles (* = $p < 0.05$, when compared to TRADM; † = $p < 0.05$, when compared to MONO; ‡ = $p < 0.05$, when compared to TRADB).

	Biarticular			Monoarticular			Total		
	Gastroc	Rec Fem	Hamst	Sol + Tib P	Vastus	Glutes	Ankle	Knee	Hip
TRADM	1.2 ± 0.4	0.4 ± 0.5	0.6 ± 0.3	3.7 ± 0.7	2.1 ± 0.4	1.9 ± 0.8	4.9 ± 1.0	2.3 ± 0.4	2.4 ± 0.8
TRADB	0.7 ± 0.3*	0.2 ± 0.1	0.7 ± 0.3	4.4 ± 1.0*	2.3 ± 0.4*	2.2 ± 0.7	5.0 ± 1.1	2.4 ± 0.4*	2.8 ± 0.9*
MONO	1.2 ± 0.3	0.5 ± 0.5	0.6 ± 0.3	3.6 ± 0.8	2.1 ± 0.4	2.0 ± 1.0	4.8 ± 1.1	2.2 ± 0.4	2.4 ± 1.0
BI	1.0 ± 0.5	0.6 ± 0.4	1.0 ± 0.5†	4.2 ± 1.4†	2.5 ± 0.5†	2.9 ± 1.2†	5.0 ± 1.5	2.5 ± 0.5†	3.5 ± 1.5†
BIH	1.0 ± 0.6‡	0.6 ± 0.4‡	1.0 ± 0.5†‡	4.2 ± 1.4†	2.5 ± 0.5†‡	2.9 ± 1.1†‡	5.0 ± 1.5	2.5 ± 0.5†	3.5 ± 1.6†‡

Note: total represents the peak muscle force for biarticular and monoarticular muscles combined.

Table 2. Peak muscle forces (× BW) calculated during landing for selected muscles (* = $p < 0.05$, when compared to TRADM; † = $p < 0.05$, when compared to MONO; ‡ = $p < 0.05$, when compared to TRADB).

	Biarticular			Monoarticular			Total		
	Gastroc	Rec Fem	Hamst	Sol + Tib P	Vastus	Glutes	Ankle	Knee	Hip
TRADM	1.1 ± 0.6	0.7 ± 0.7	0.5 ± 0.3	3.6 ± 1.4	2.2 ± 0.5	1.6 ± 1.0	4.6 ± 1.8	2.4 ± 0.6	1.9 ± 1.0
TRADB	1.0 ± 0.5	0.6 ± 0.4	0.5 ± 0.3	3.9 ± 1.6	2.4 ± 0.5*	2.0 ± 1.5	4.6 ± 1.6	2.6 ± 0.5*	2.3 ± 1.6
MONO	1.2 ± 0.6	0.7 ± 0.7	0.5 ± 0.3	3.7 ± 1.4	2.2 ± 0.6	1.7 ± 1.0	4.8 ± 1.9	2.4 ± 0.6	1.9 ± 1.0
BI	1.5 ± 0.5†	1.3 ± 0.6†	0.9 ± 0.6†	4.0 ± 2.0	2.7 ± 0.6†	2.4 ± 1.7†	5.0 ± 2.4	2.9 ± 0.6†	2.9 ± 2.1†
BIH	1.6 ± 0.8†‡	1.3 ± 0.6‡	1.0 ± 0.6†‡	4.0 ± 2.0	2.7 ± 0.7†‡	2.4 ± 1.7†	5.2 ± 2.6	2.9 ± 0.7†‡	3.0 ± 2.1†

Note: total represents the peak muscle force for biarticular and monoarticular muscles combined.

Table 3. Mean peak joint forces (× BW) calculated during vertical jumping (* = $p < 0.05$, when compared to TRADM; † = $p < 0.05$, when compared to MONO; ‡ = $p < 0.05$, when compared to TRADB).

	Ankle	Knee				Hip
		PFJ	TFJ	AS	PS	
TRADM	8.7±1.7	4.2±1.3	7.0±1.9	0.4±0.3	0.8±0.8	4.6±1.2
TRADB	9.1±1.8*	4.5±1.3*	8.1±2.0*	0.4±0.3	1.0±0.7	5.8±1.3*
MONO	8.6±1.7	4.1±1.3	7.0±2.0	0.4±0.3	1.0±0.9	4.8±1.3
BI	9.2±1.9†	4.5±1.2†	8.4±2.2†	0.7±0.5†	1.5±1.0†‡	6.8±1.5†‡
BIH	9.2±1.9†	4.5±1.2†	8.4±2.1†	0.7±0.5†	1.5±1.0†‡	6.8±1.5†‡

Table 4. Mean peak joint forces (× BW) calculated during landing (* = $p < 0.05$, when compared to TRADM; † = $p < 0.05$, when compared to MONO; ‡ = $p < 0.05$, when compared to TRADB).

	Ankle	Knee				Hip
		PFJ	TFJ	AS	PS	
TRADM	8.2±2.9	3.6±1.0	7.6±3.8	0.6±0.3	0.7±0.5	5.2±2.7
TRADB	8.5±3.1	3.8±0.9*	8.3±3.6*	0.6±0.3	0.7±0.4	5.8±3.0
MONO	8.5±3.2	3.6±1.0	7.5±3.7	0.6±0.3	0.7±0.6	5.2±2.7
BI	9.4±4.7	4.0±1.0†‡	9.6±4.8†‡	0.7±0.4	1.0±0.9†	7.2±3.1†‡
BIH	9.6±4.8†	4.0±1.1†‡	9.7±4.9†‡	0.7±0.4	1.1±1.0	7.3±3.2†‡

Table 5. Mean peak muscle power (W/kg) of selected biarticular muscles during vertical jumping (‡ = $p < 0.05$, when compared to TRADB).

	Gastrocnemius		Rectus Femoris		Hamstrings	
	Max	Min	Max	Min	Max	Min
TRADB	4.4 ± 4.7	-0.4 ± 0.1	1.6 ± 1.0	-0.2 ± 0.1	2.0 ± 1.0	-0.7 ± 0.5
BI	4.0 ± 2.7	-0.7 ± 0.6	5.2 ± 3.7‡	-0.3 ± 0.2	4.0 ± 2.0‡	-0.6 ± 0.5
BIH	4.0 ± 2.7	-0.7 ± 0.6	5.2 ± 3.7‡	-0.3 ± 0.2	4.0 ± 2.0‡	-0.6 ± 0.5

Table 6. Mean peak muscle power (W/kg) of selected biarticular muscles during landing (‡ = $p < 0.05$, when compared to TRADB).

	Gastrocnemius		Rectus Femoris		Hamstrings	
	Max	Min	Max	Min	Max	Min
TRADB	1.0 ± 0.7	-5.7 ± 4.0	0.1 ± 0.1	-2.6 ± 1.9	0.3 ± 0.2	-1.8 ± 1.2
BI	1.8 ± 1.2‡	-6.3 ± 3.0	0.1 ± 0.2	-5.6 ± 2.1‡	0.3 ± 0.3	-3.7 ± 2.9‡
BIH	1.9 ± 1.3‡	-6.3 ± 3.0	0.1 ± 0.2	-5.7 ± 2.2‡	0.3 ± 0.3	-3.7 ± 2.9‡

Table 7. Mean peak sagittal plane extension moments (Nm/kg) calculated during vertical jumping and landing (* = $p < 0.05$, when compared to TRAD).

	Jumping			Landing		
	Ankle	Knee	Hip	Ankle	Knee	Hip
TRAD	-1.56±0.14	1.65±0.23	-1.55±0.24	-1.58±0.35	1.78±0.51	-1.04±0.46
MONO	-1.56±0.14	1.65±0.23	-1.55±0.24	-1.58±0.35	1.78±0.51	-1.04±0.46
BI	-1.56±0.14	1.70±0.25*	-2.23±0.83*	-1.58±0.35	1.91±0.48*	-1.52±0.74
BIH	-1.56±0.14	1.70±0.25*	-2.23±0.83*	-1.58±0.35	1.91±0.48*	-1.52±0.75

Figure Legends

Figure 1. The relationship between monoarticular and biarticular muscles in creating joint moments.

Figure 2. Nomenclature used in the 1 and 2 step approaches for segment i.

Figure 3. Internal knee forces.

Figure 4. Selected muscle forces for a typical subject (subject 12) based on the TRADM, TRADB and BI methods.

Figure 5. Muscle power of selected biarticular muscles for a typical subject (subject 12) based upon the TRADB and BI methods.

Figure 6. Sagittal plane moments during vertical jumping and landing (subject 12).

Figure 7. Moment equilibrium in the 1 and 2 step approaches.

Table Legends

Table 1. Peak muscle forces (× BW) calculated during vertical jumping for selected muscles (* = $p < 0.05$, when compared to TRADM; † = $p < 0.05$, when compared to MONO; ‡ = $p < 0.05$, when compared to TRADB).

Table 2. Peak muscle forces (× BW) calculated during landing for selected muscles (* = $p < 0.05$, when compared to TRADM; † = $p < 0.05$, when compared to MONO; ‡ = $p < 0.05$, when compared to TRADB).

Table 3. Mean peak joint forces (× BW) calculated during vertical jumping (* = $p < 0.05$, when compared to TRADM; † = $p < 0.05$, when compared to MONO; ‡ = $p < 0.05$, when compared to TRADB).

Table 4. Mean peak joint forces (× BW) calculated during landing (* = $p < 0.05$, when compared to TRADM; † = $p < 0.05$, when compared to MONO; ‡ = $p < 0.05$, when compared to TRADB).

Table 5. Mean peak muscle power (W/kg) of selected biarticular muscles during vertical jumping (‡ = $p < 0.05$, when compared to TRADB).

Table 6. Mean peak muscle power (W/kg) of selected biarticular muscles during landing (‡ = $p < 0.05$, when compared to TRADB).

Table 7. Mean peak sagittal plane extension moments (Nm/kg) calculated during vertical jumping and landing (* = $p < 0.05$, when compared to TRAD).

Table of Abbreviations

Abbreviation	Definition
AS	Anterior tibial shear
BI	Inverse optimization approach (biarticular muscles with standard upper bounds)
BIH	Inverse optimization approach (selected biarticular muscles have double the standard upper bound)
GCS	Global coordinate system
LCS	Local coordinate system
MONO	Inverse optimization approach (only monoarticular muscles)
PFJ	Patellofemoral joint contact force
PS	Posterior tibial shear
TFJ	Tibiofemoral joint contact force
TRAD	Traditional method of calculating joint moments
TRADB	Traditional method of calculating muscle forces (biarticular muscles with standard upper bounds)
TRADM	Traditional method of calculating muscle forces (only monoarticular muscles)

Figure 1. The relationship between monoarticular and biarticular muscles in creating joint moments.

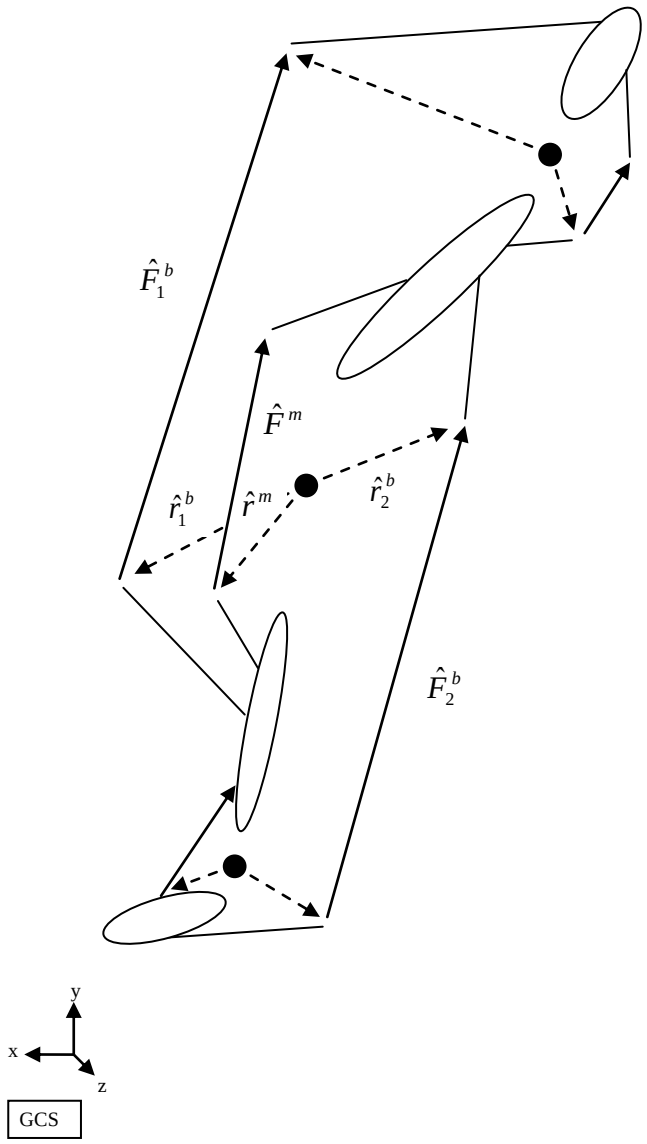

Note: diagram depicts muscle wrapping points. Line of action of muscle is taken from effective insertion to effective origin. Moment arm is taken from centre of rotation to effective insertion on the rotated segment.

Figure 2. Nomenclature used in the 1 and 2 step approaches for segment i.

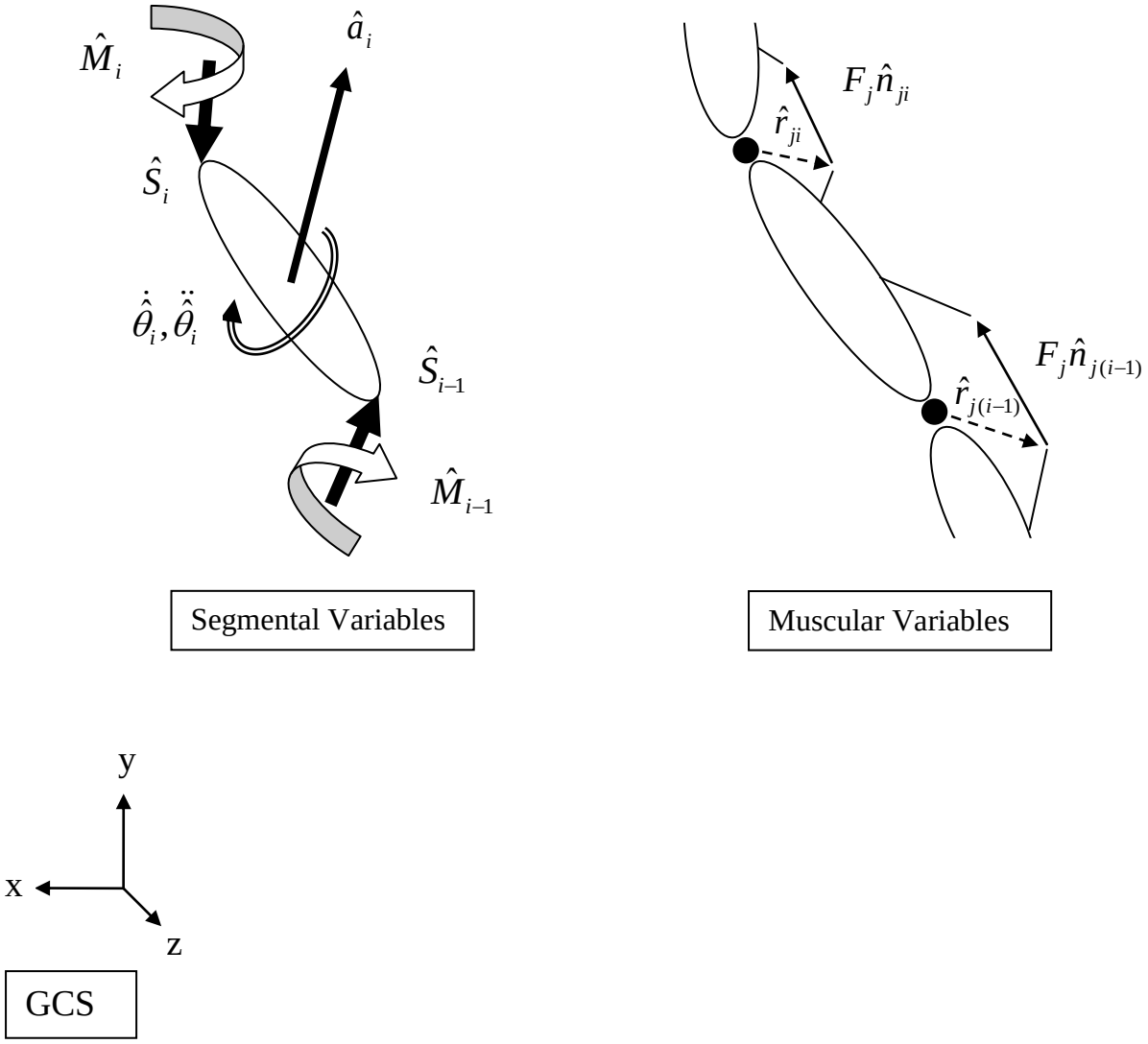

Figure 3. Internal knee forces.

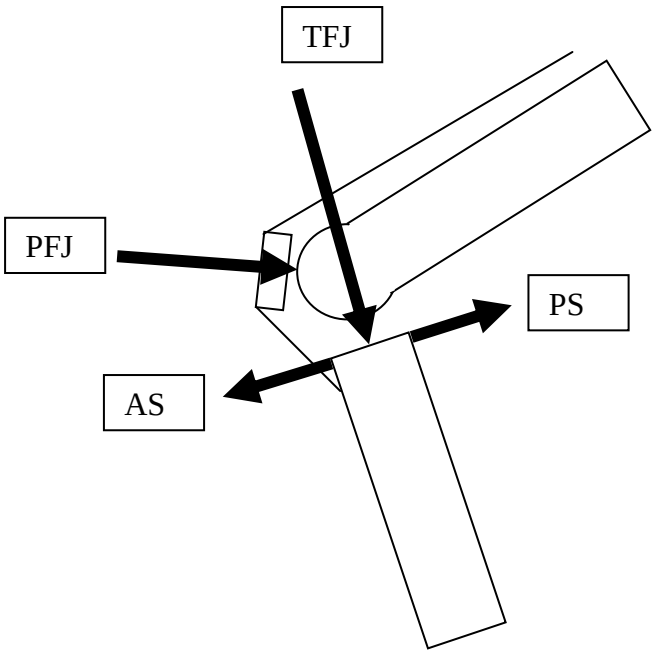

Figure 4. Selected muscle forces for a typical subject (subject 12) based on the TRADM, TRADB and BI methods.

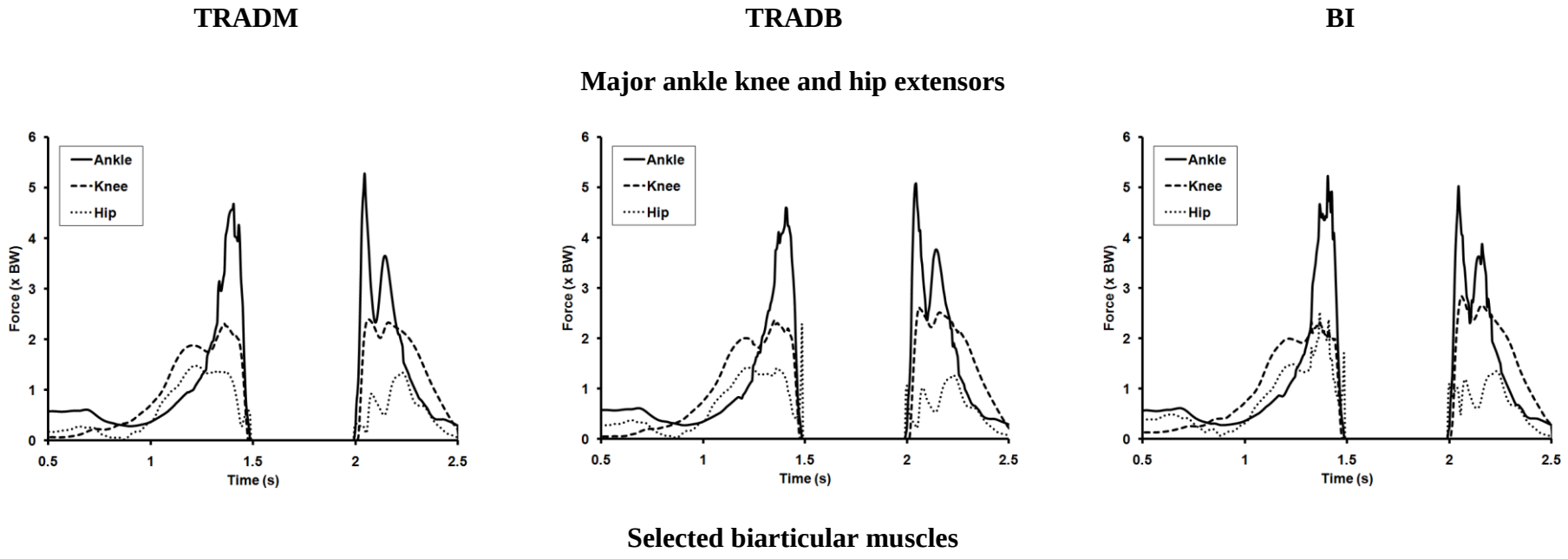

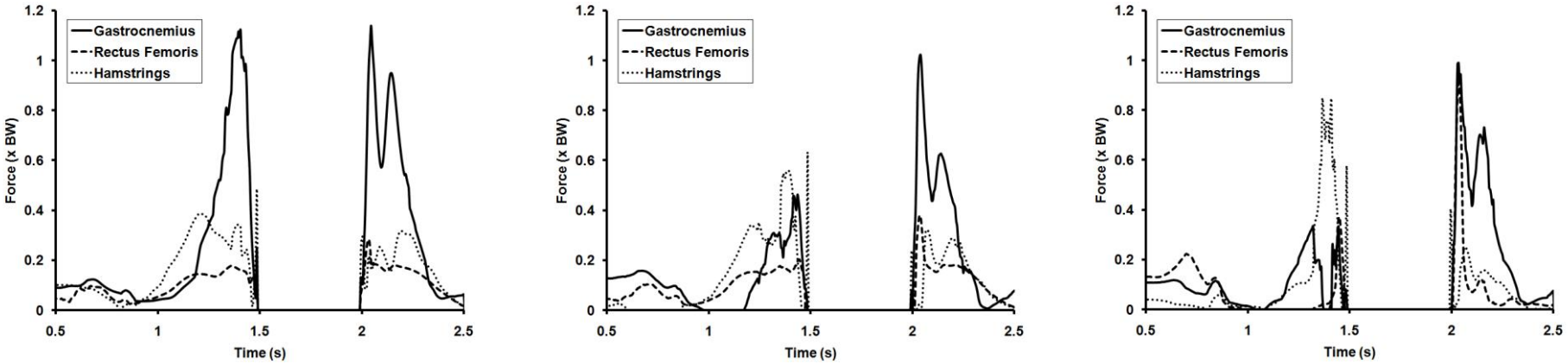

Selected monoarticular muscles

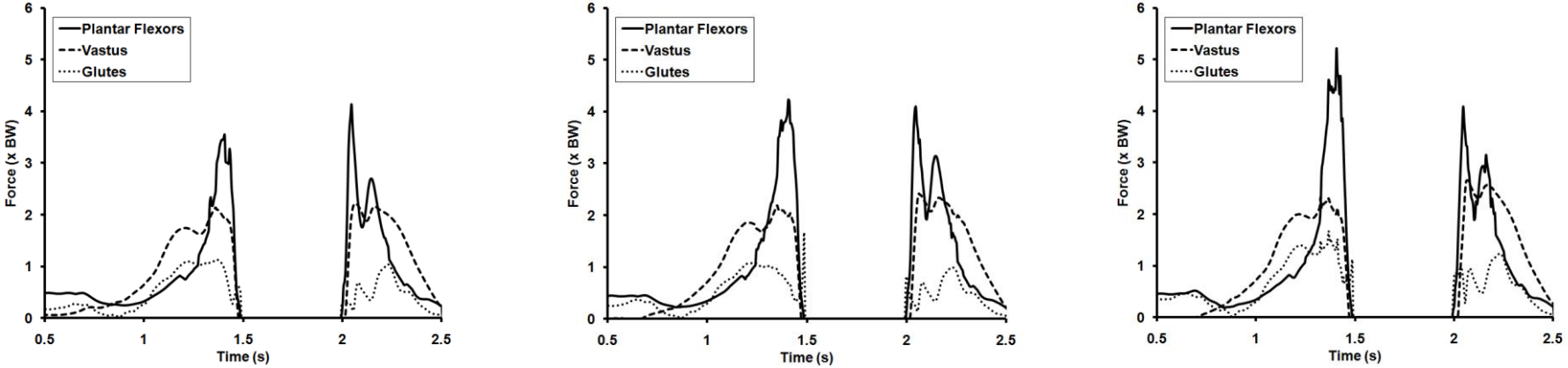

Figure 5. Muscle power of selected biarticular muscles for a typical subject (subject 12) based upon the TRADB and BI methods.

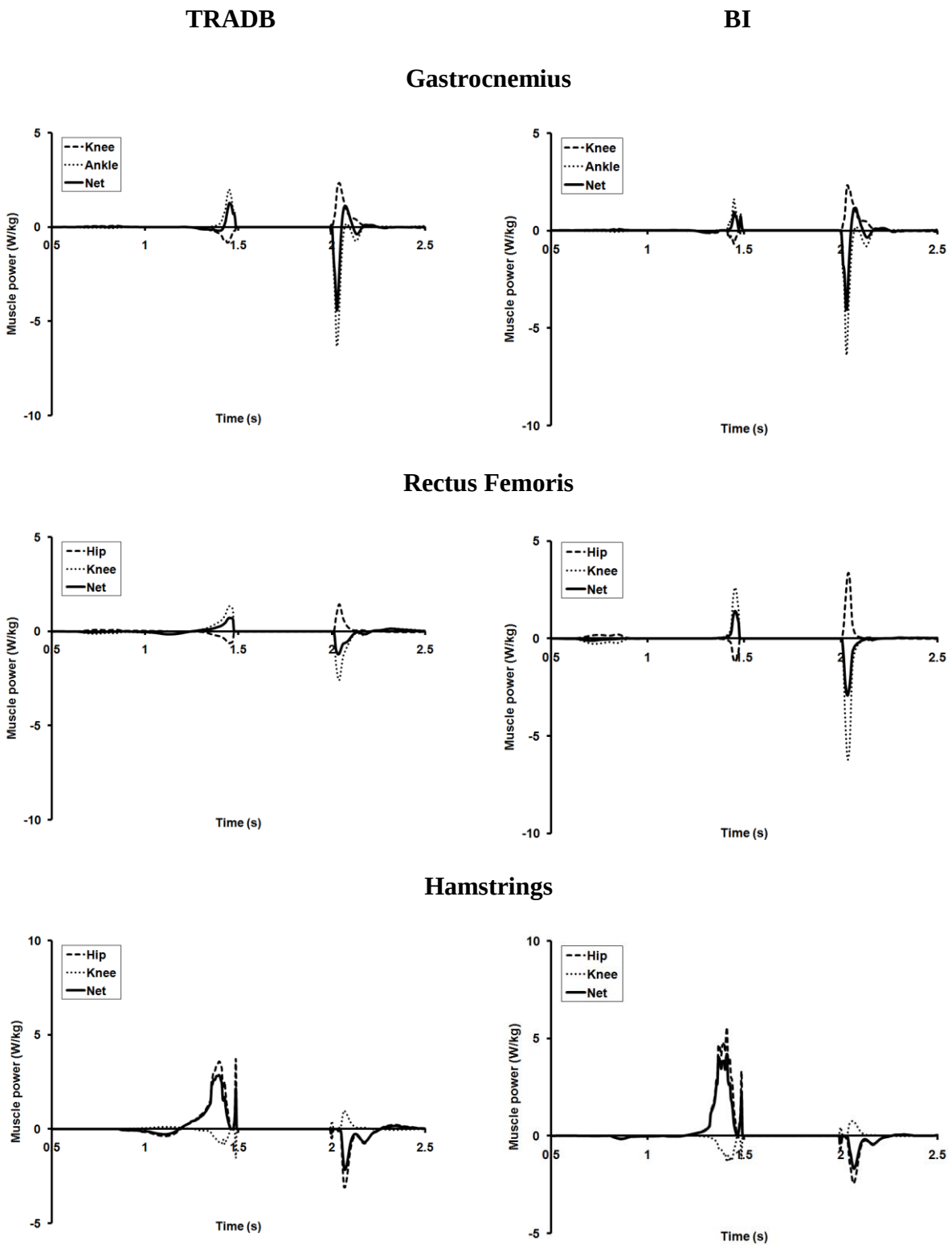

Figure 6. Sagittal plane moments during vertical jumping and landing (subject 12).

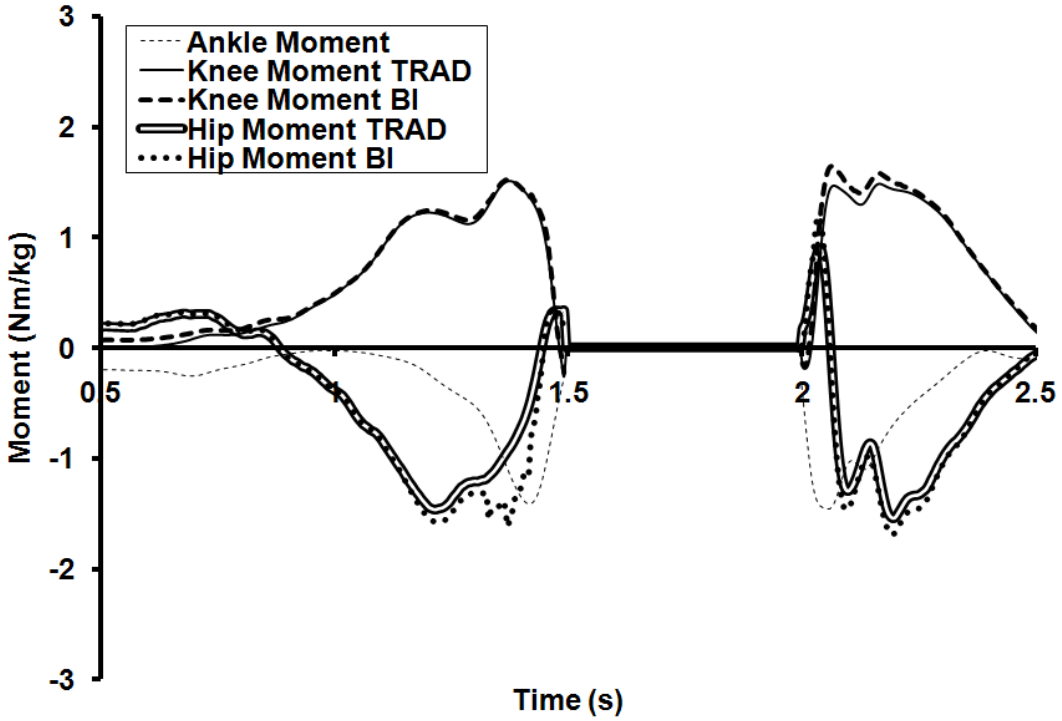

Figure 7. Moment equilibrium in the 1 and 2 step approaches.

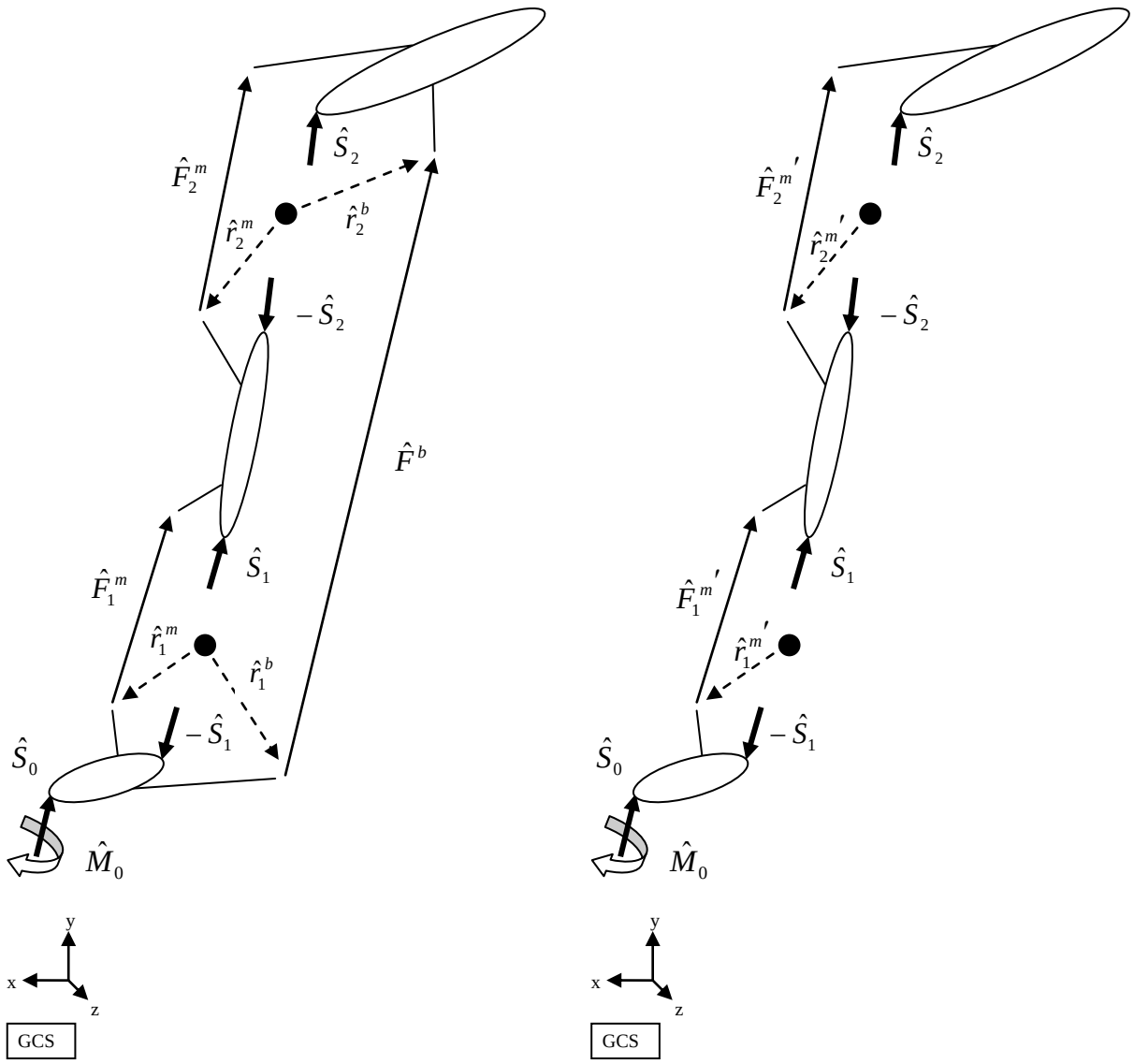

Note: diagram depicts muscle wrapping points. Line of action of muscle is taken from effective insertion to effective origin. Moment arm is taken from centre of rotation to effective insertion on the rotated segment.